A ceria based conversion coating on squeeze cast Mg- 4wt. %Y alloy for improved corrosion resistance in 0.1 M NaCl solution

Presented by

Partha Saha *, Meeta Kamde and Yogendra Mahton

Department of Ceramic Engineering
National Institute of Technology Rourkela
Odisha-769008, India

Why magnesium…???

- **Magnesium (Mg)** is the 6th most abundant element and the **lightest structural material** present on the Earth's surface.

- It has **high specific strength**, **excellent damping capabilities**, **good castability**, **excellent machinability**, **good electromagnetic shielding**, and **recyclability**.

- However, Mg has poor **high temperature mechanical properties (creep)** and limited **salt-water corrosion resistance,** which decreases its widespread application in engineering materials.

Applications

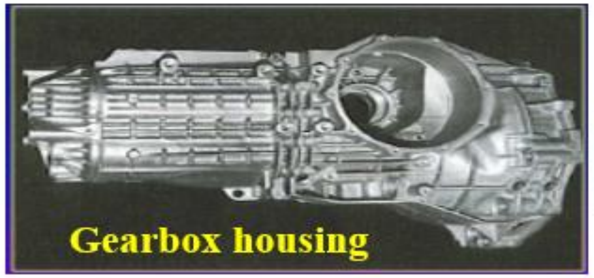

Alloyed wheel

G. Song and A. Atrens, "*Advanced Engineering Materials*", 2003, 5(12): p. 837-858
Kelvii Wei Guo, "*Recent Patents on Corrosion Science*", 2010, 2: p. 13-21

E(potential) vs. pH stability diagram of magnesium

Mg alloys are **extremely susceptible** to galvanic corrosion, which can cause **severe pitting** in the metal resulting in decreased mechanical stability.

Thermodynamically Mg is very active and prone to oxidation, standard Gibbs free energy (ΔG^0) for the following oxidation reactions are negative.

$Mg^{2+} + 2OH^- = Mg(OH)_2$, ($\Delta G^0$) = -833 kJ/mol ……(1)

$Mg + ½ O_2 = MgO$, (ΔG^0) = -569 kJ/mol …….(2)

$Mg + 2H_2O = Mg(OH)_2 + H_2$, ($\Delta G^0$) = -359 kJ/mol …......(3)

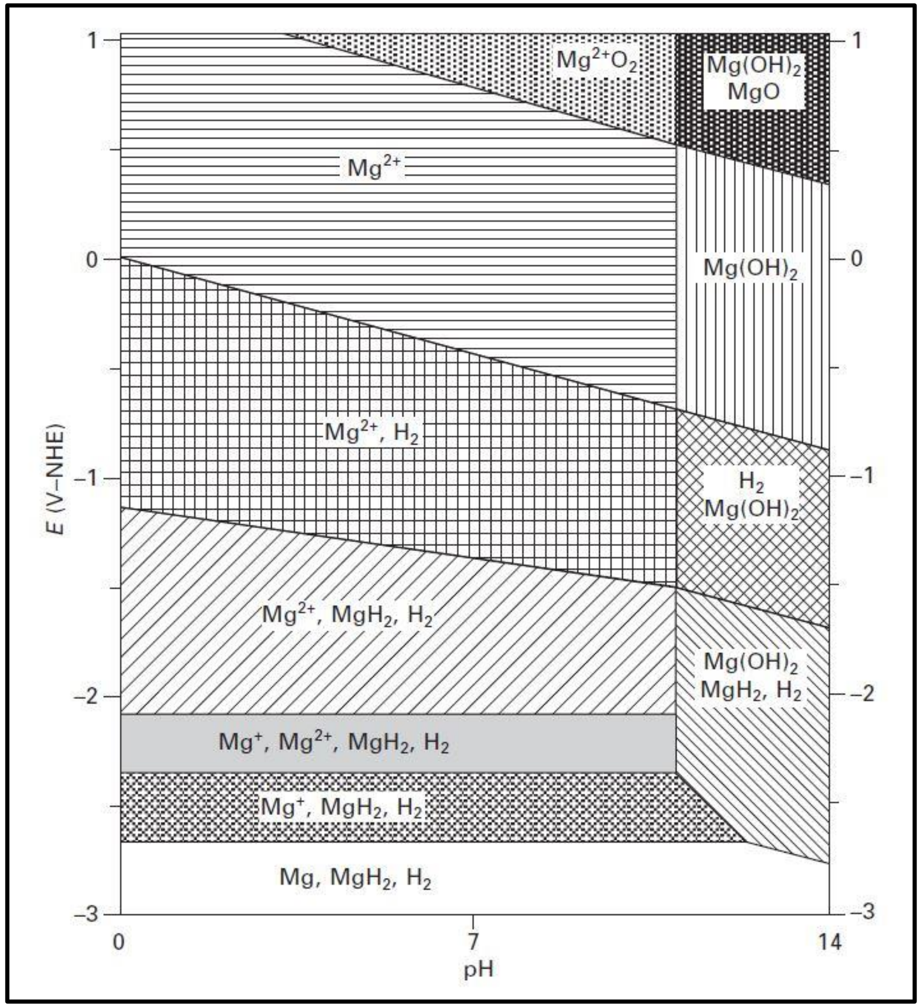

E–pH diagram with possible stable substances in a Mg–H_2O electrochemical system.

Prevention of corrosion in magnesium

- **Alloying additions**
- **Keeping the impurities below tolerance level**
- **Electrodeposition methods**
- **Conversion and/or electrophoretic coatings**
- **Anodization of Mg alloys**

A. Atrens et al., "*Advanced Engineering materials*", 2015, 4(17): p. 400-453

Objectives

- Development of Mg based alloys using Y as alloying addition within their permissible maximum solid solubility limits by squeeze casting.

- Determine the microstructures and mechanical properties.

- Perform Cerium conversion coating (CeCC) on Mg-4wt.%Y samples for different time periods.

- Examine the influence of surface films formed on Mg alloys by open-circuit corrosion in 0.1 molar NaCl solution by electrochemical and immersion corrosion methods.

- Perform XRD, SEM/EDS on the samples to determine mechanical properties before and after salt-water corrosion to monitor the growth processes of surface films during open-circuit corrosion and the subsequent polarization experiment in 0.1 molar NaCl solutions.

Experimental procedure

Mg-4.0 wt.% alloy was developed using a bottom pouring type stir casting furnace with squeeze casting setup (Swamequip, Chennai, India)

Materials used

99.99% Pure Magnesium ingot (Minex Metallurgical Ltd. Pune)

Mg-30 wt.% Y master alloy (China Human High Board Materials)

Preheating of furnace to 750°C

↓

Addition of Pure Magnesium ingot and Mg-30 wt.% Yttrium master alloy

↓

Complete melting of both the ingots

↓

Melt stirring at 750°C

↓

Pouring of melt in the mould

Flow of Ar and SF_6 gas mixture → Complete melting of both the ingots; Melt stirring at 750°C; Pouring of melt in the mould

Application of squeeze pressure → Pouring of melt in the mould

Mg-4 wt.%Y ingot

Fig. Bottom pouring type stir casting furnace with squeeze casting setup

- Squeeze casting set-up combines the advantages of casting and forging process .
- Prevention of gas and shrinkage due to rapid solidification by pressure applied.
- Offers fine microstructures with higher strength components.

Flow chart of CeCC on Magnesium specimen

Samples were cut into 10 mm x 10 mm x 2mm dimension and polished with 320 and 1200 grit SiC paper

↓

Polished samples were cleaned ultrasonically with propanol & rinsed with DI water & dried at room temperature

↓

Cleaned samples were coated with 0.05 M $Ce(NO_3)_3.6H_2O$ and 0.254 M H_2O_2 at room temperature with pH=2.9 (For time- 30, 60, 120 and 1800 s)

↓

Coated samples were then post-treated in 2.5 wt.% NaH_2PO_4 aqueous solution for 5 minutes at 85 °C

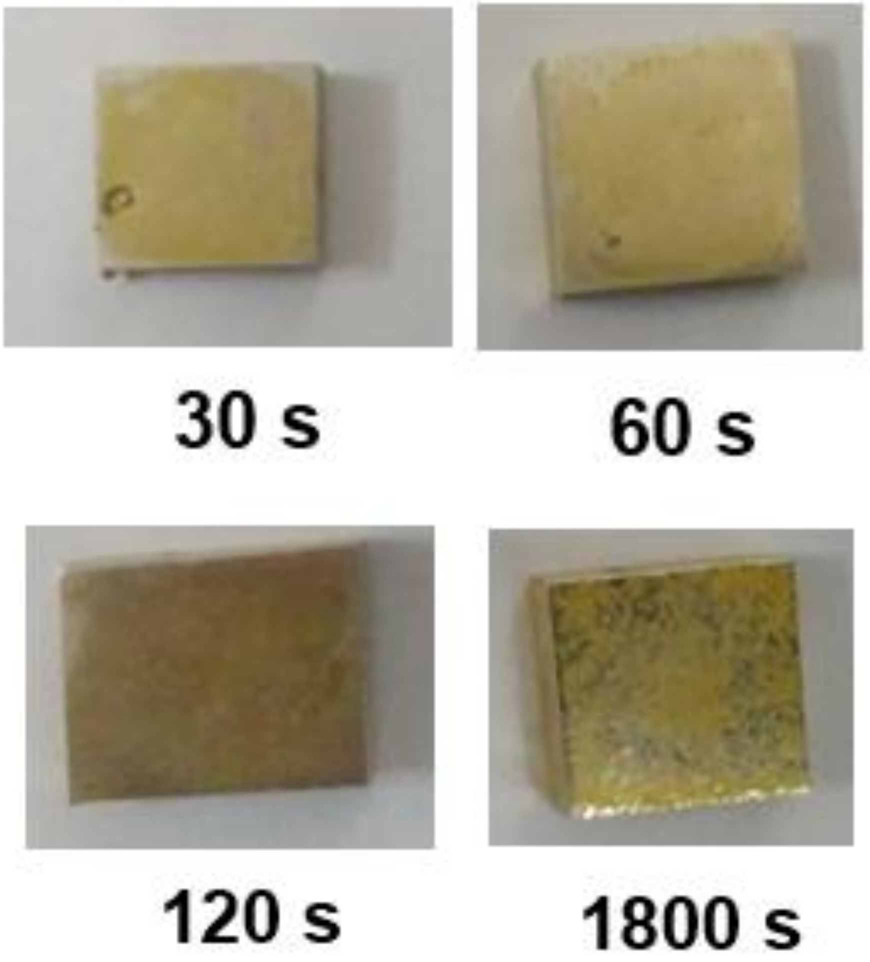

CeCC on Mg-4Y samples for 30, 60, 120 and 1800s

XRD analysis of CeCC on Mg-4Y samples

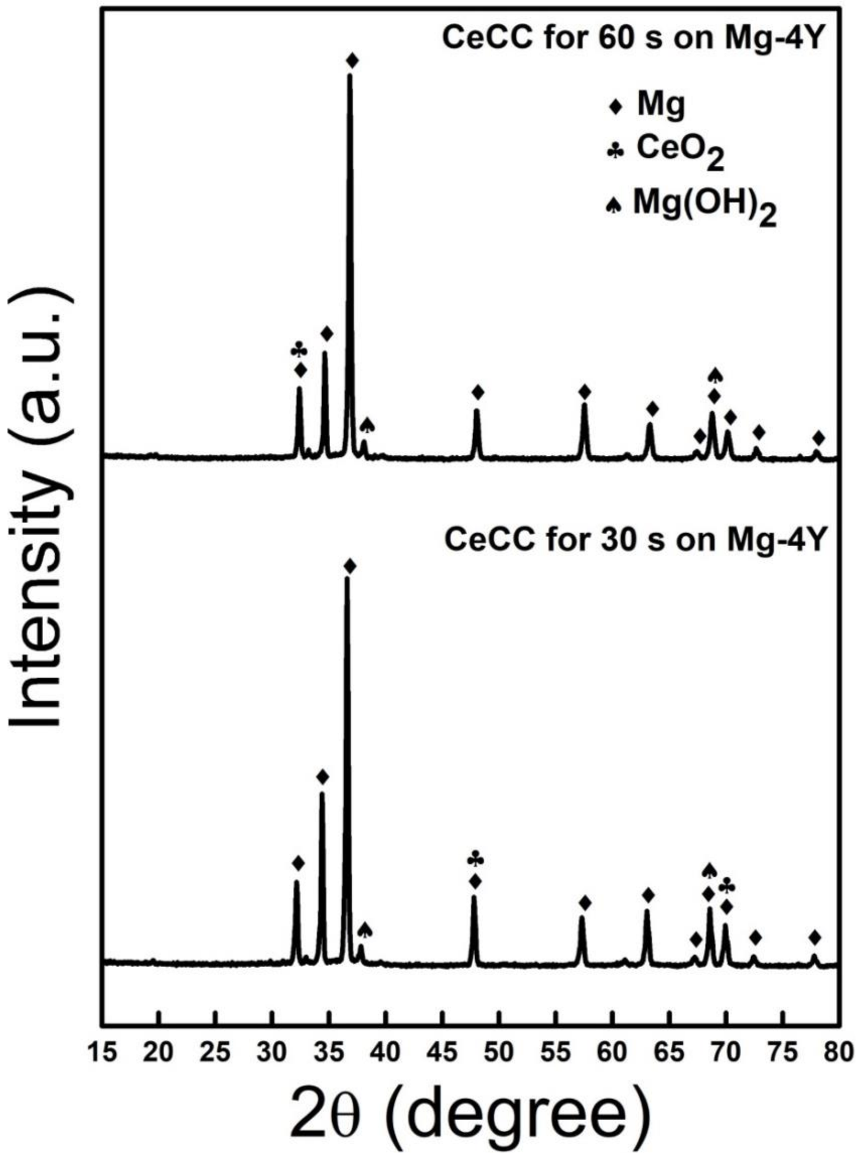

The base metal peaks appeared at high intensity along with the low intensity peaks of CeO_2 and $Mg(OH)_2$ confirming the presence of CeO_2 deposition on the base metal.

ATR-FTIR plots of CeCC on Mg-4Y samples

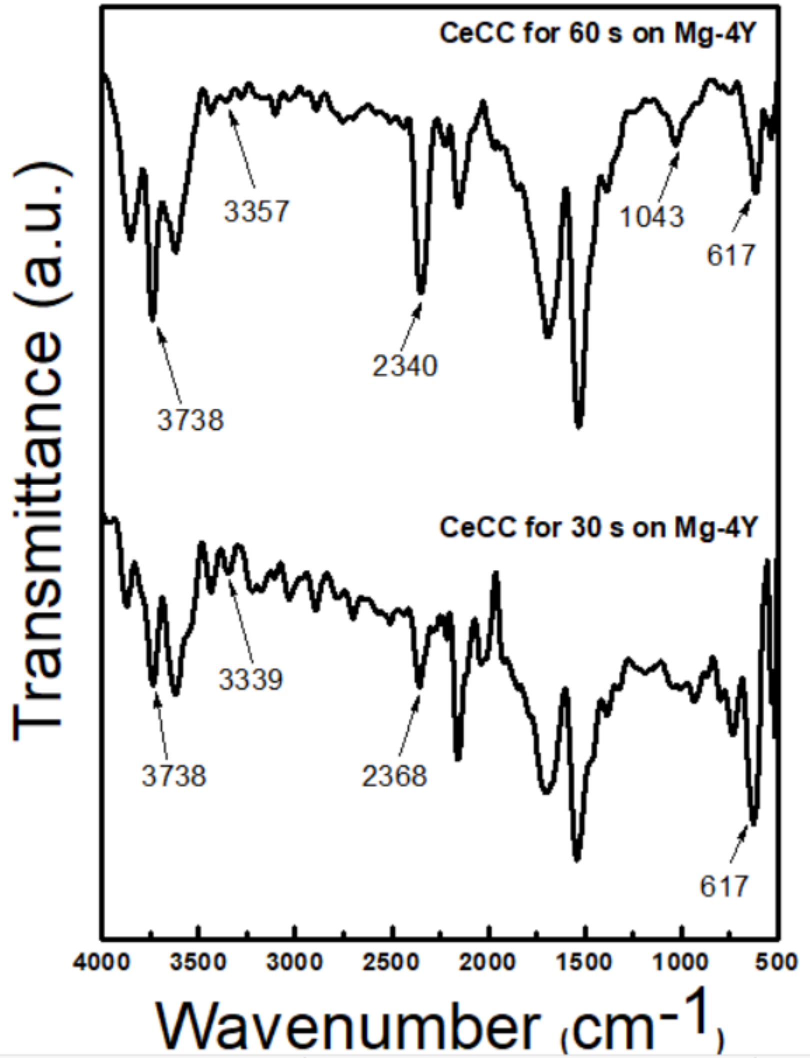

Wavenumber (cm^{-1})	Functional groups
617	Stretching vibration of Ce-O band
1034	Stretching band of C-O
1500	Mg-O
2340	C-H stretching vibration
3357	OH stretching vibration peak
3738	Stretching vibration of hydroxyl group

Presence of CeO_2 and $Mg(OH)_2$ has been validated with functional groups

Microstructure and morphology of CeCC on Mg-4Y alloy

CeCC for 30 s

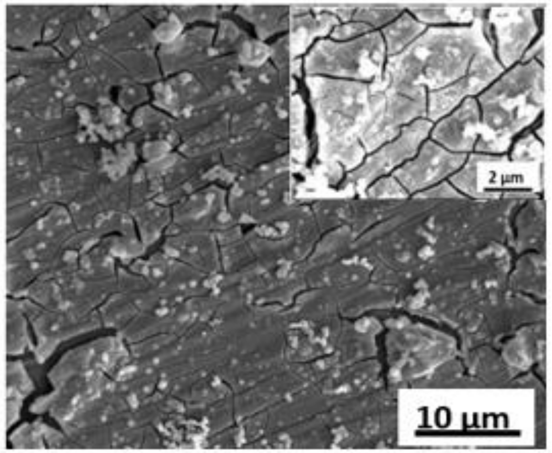

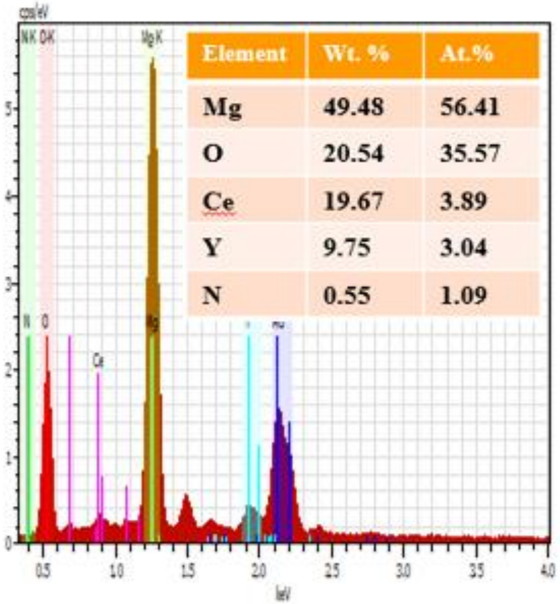

Element	Wt. %	At.%
Mg	49.48	56.41
O	20.54	35.57
Ce	19.67	3.89
Y	9.75	3.04
N	0.55	1.09

CeCC for 60 s

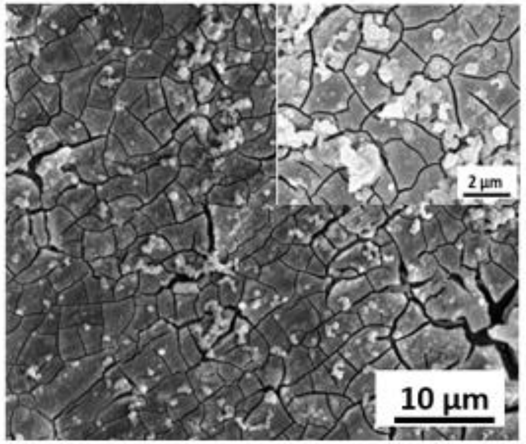

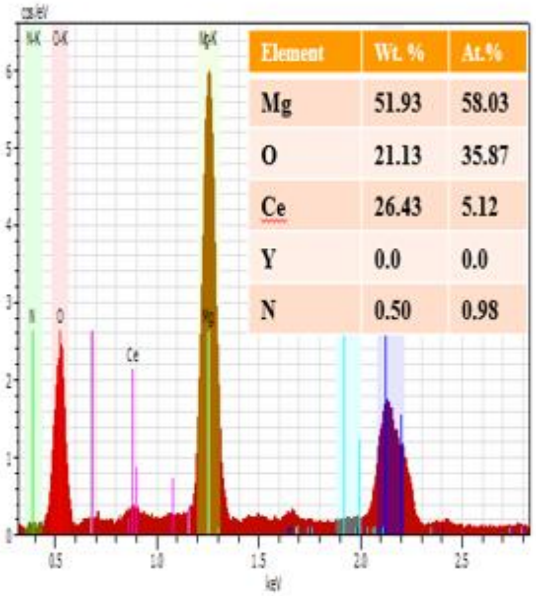

Element	Wt. %	At.%
Mg	51.93	58.03
O	21.13	35.87
Ce	26.43	5.12
Y	0.0	0.0
N	0.50	0.98

CeCC for 120 s

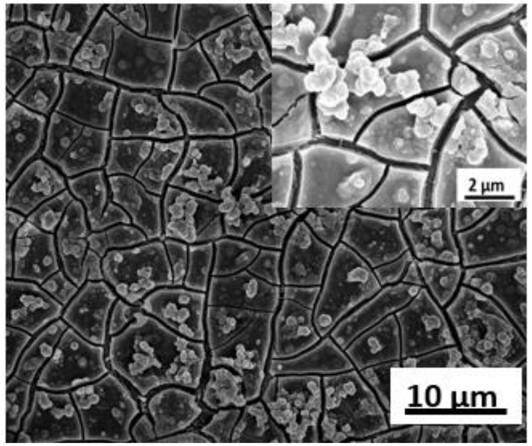

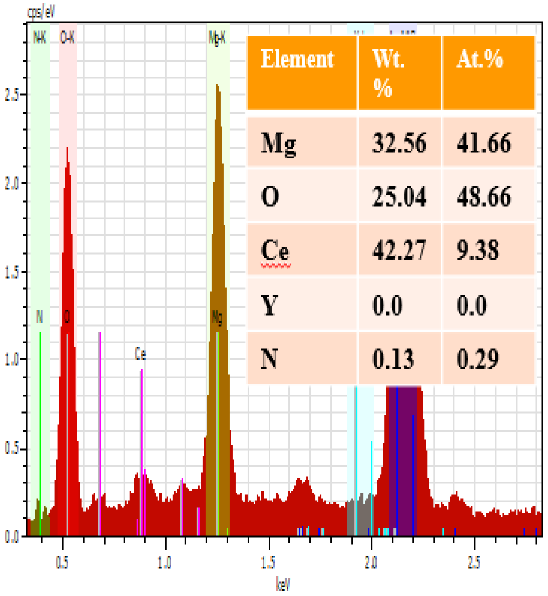

Element	Wt. %	At.%
Mg	32.56	41.66
O	25.04	48.66
Ce	42.27	9.38
Y	0.0	0.0
N	0.13	0.29

CeCC for 1800s

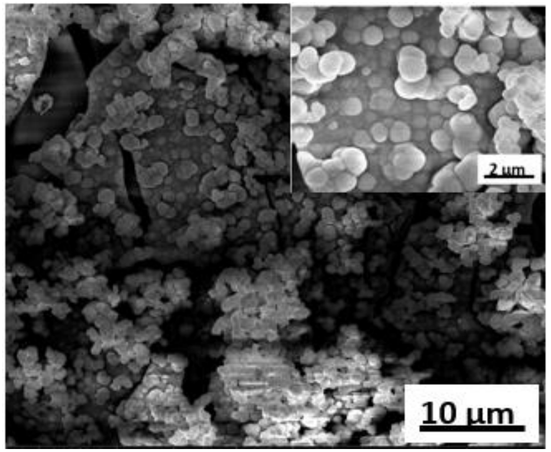

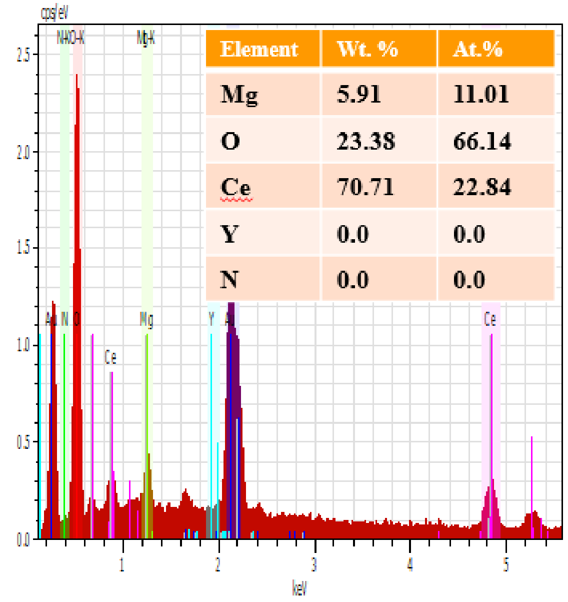

Element	Wt. %	At.%
Mg	5.91	11.01
O	23.38	66.14
Ce	70.71	22.84
Y	0.0	0.0
N	0.0	0.0

Surface chemical composition of CeCC on Mg-4 wt.%Y alloy

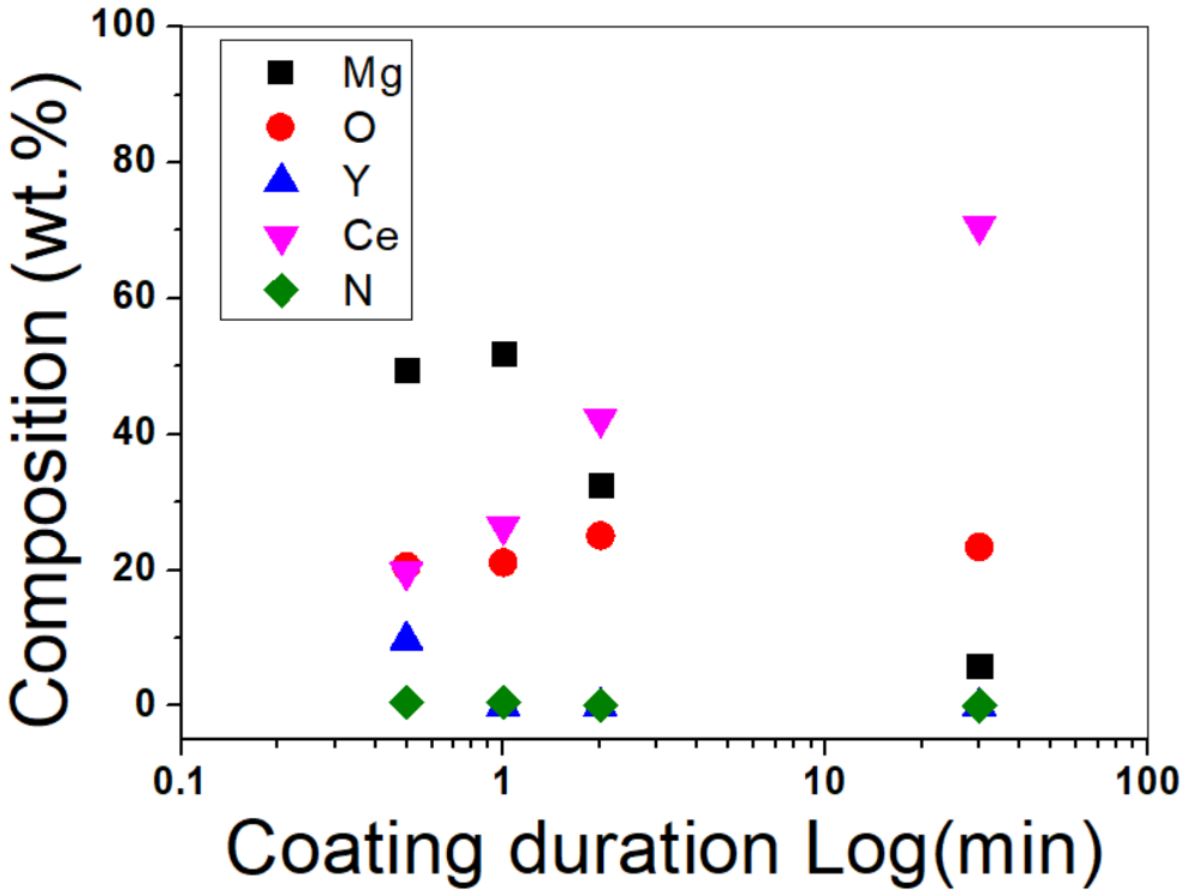

The amount of nitrogen was negligible with marginal lowering of Yttrium content throughout the coating duration. In addition, the amounts of Oxygen and Cerium were increasing with the increasing coating duration.

Furthermore, the amount of Mg gradually decreased as the coating duration was increased from 30s to 300s confirms the progressive growth of CeCC.

Surface roughness and coating thickness of CeCC

Sample ID	Surface roughness (µm)	CeCC thickness (µm)
Mg-4Y_30s	0.13 ± 0.01	1.30 ± 0.001
Mg-4Y_60s	0.32 ± 0.09	0.73 ± 0.06
Mg-4Y_120s	0.34 ± 0.18	1.03 ± 0.15
Mg-4Y_ 1800s	1.22 ± 0.03	4.20 ± 0.54

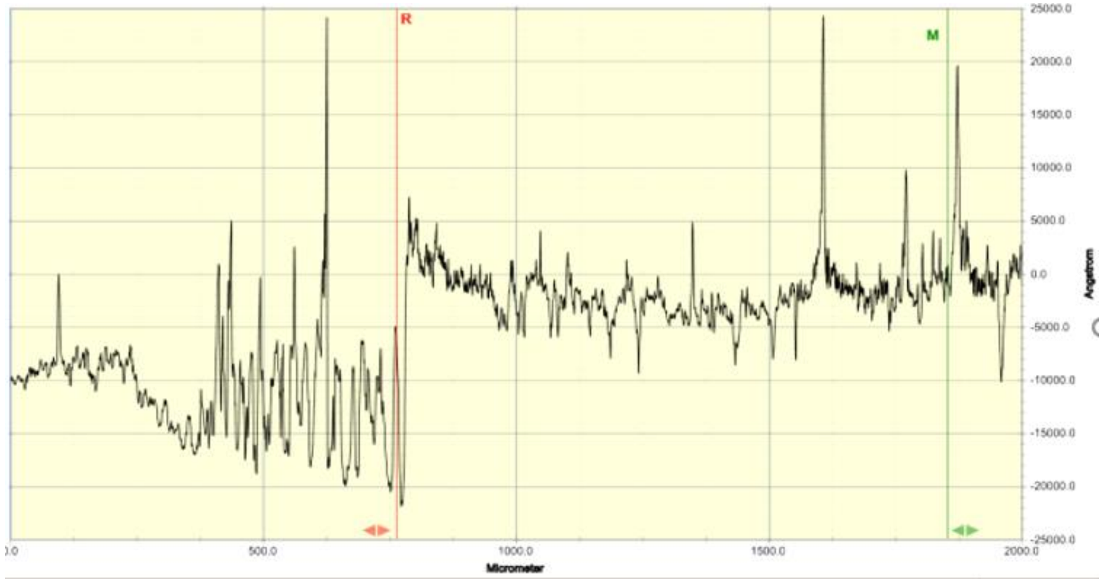

Image showing the graphical representation for CeCC for 30s on Mg-4Y sample using stylus surface profilometer

The coating thickness was found minimum in Mg-4Y_60s and maximum for Mg-4Y_1800s sample.

Corrosion Testing

Immersion test

The immersion corrosion test were performed on both the bare and CeCC Mg-4Y samples, taking specimens of 10 ×10 × 2 mm^3, and immersed in a 0.1 M NaCl solution at 25°C for 8h. The change of pH was recorded after each hour with a standard pH-meter. The samples after immersion were cleaned using a solution having (20% Cr_2O_3 + 1% $AgNO_3$) to remove the corrosion products. From the weight difference of the samples before and after corrosion, the corrosion rate was calculated.

pH and corrosion rate obtained after static immersion in 0.1 M NaCl for 8 h

- The corrosion rate was calculated according to ASTM G 31-72. Mg-4Y_bare samples showed maximum corrosion rate whereas Mg-4Y_30 s samples showed the minimum corrosion rates implying that the CeCC helped in reducing corrosion in Mg alloys.

- With increasing immersion time, the pH increased towards the basic nature, and Mg-4Y_1800s sample showed highest increase in pH and Mg-4Y_bare and Mg-4Y_30s samples showed minimum increase in pH values.

Sample name	Corrosion rate (mm/year)
Mg-4wt.% Y-Bare	7.22 ± 0.33
Mg-4wt.% Y-30 s	3.09 ± 0.79
Mg-4wt.% Y-60 s	3.85 ± 0.58
Mg-4wt.% Y-120 s	3.68 ± 0.97
Mg-4wt.% Y-1800 s	4.17 ± 2.31

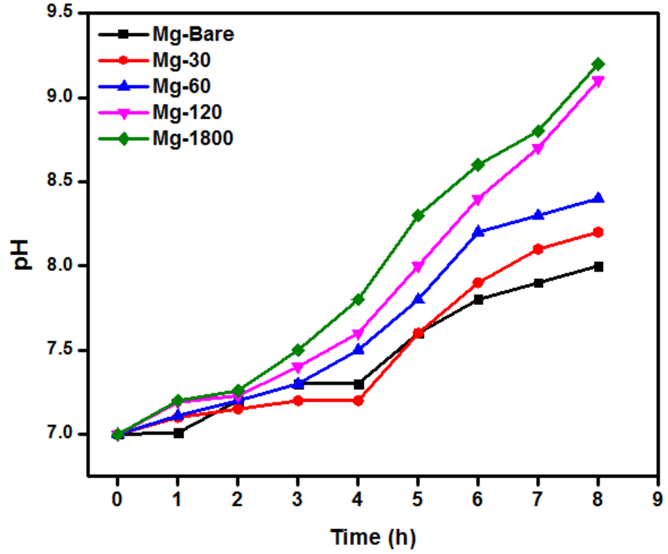

XRD analysis of corroded samples in 0.1M NaCl solution

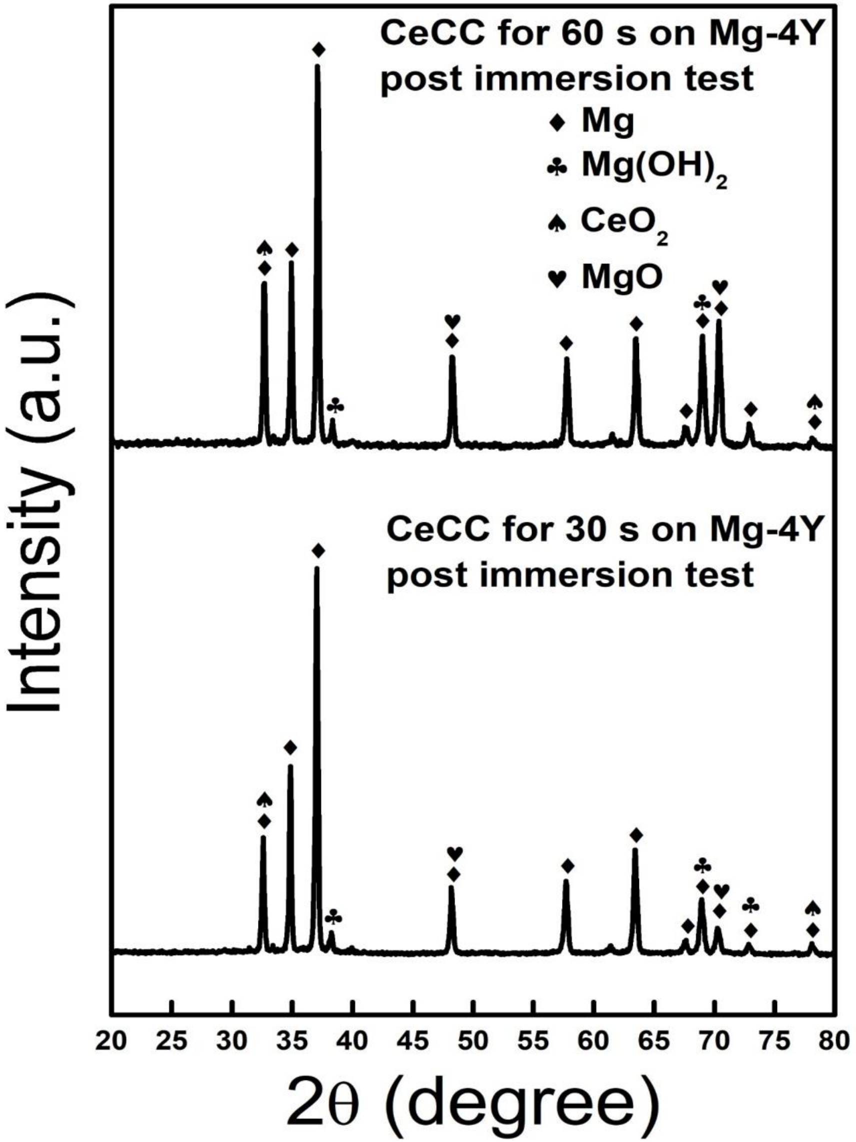

The XRD patterns showed high intensity base metal peaks along with the low intensity peaks of CeO_2 confirming the presence of CeO_2 deposition on the base metal surface with the formation of oxides (MgO and $Mg(OH)_2$) on Mg after corrosion.

Morphology of the corroded samples after post immersion test in 0.1 M NaCl

Mg-4Y_Bare

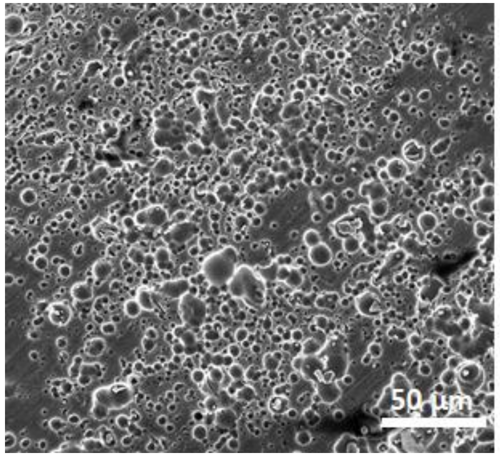

Mg-4Y_60 s

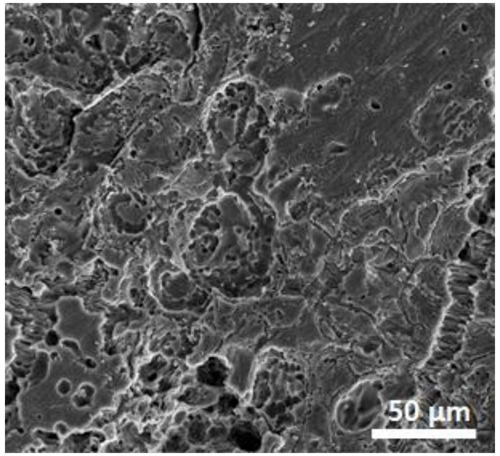

Mg-4Y_1800 s

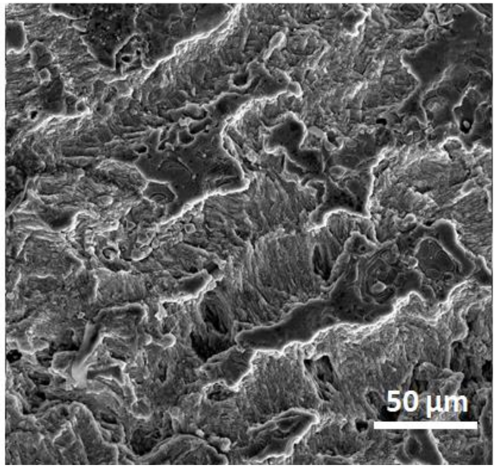

Mg-4Y_30 s

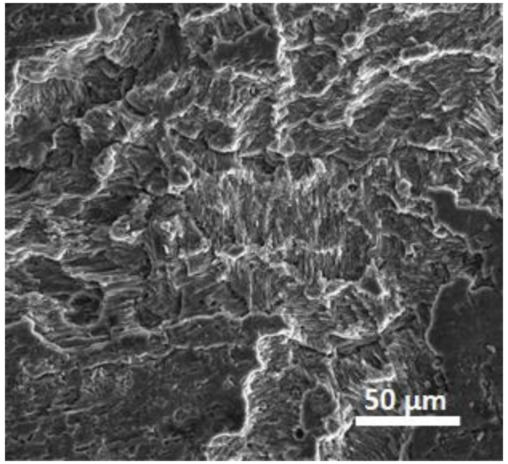

Mg-4Y_120 s

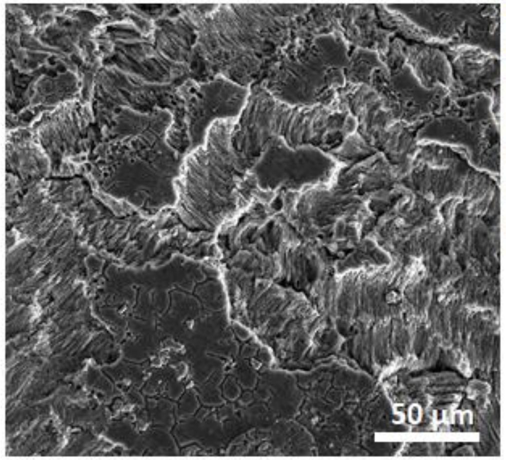

For the bare Mg-4Y sample, corrosion pits were formed with adjoining boundaries on the surface.

For the CeCC samples some sunken places appeared and tiny crevices in the film.

For the Mg-4Y_30s samples, crevices appeared but as the CeCC duration increased the crevices aggressively started penetrating in the alloy underneath and started forming deep corrosion pits.

Note: Samples were cleaned with the solution containing 20% CrO_3 and 1% $AgNO_3$ after the immersion test

Proposed reaction mechanism for CeO_2 formation

$Ce^{3+} + 2H_20 = Ce(OH)_2^{2-} + 2H^+ + e^-$ ……….(1)

$H_2O_2 + 2e^- = 2(OH)^-$ ……….(2)

Reaction (1) and (2) combines to give the following reaction as

$2Ce^{3+} + 2H_2O + H_2O_2 = 2Ce(OH)_2^{2+} + 2H^+$ ……….(3)

In the solution comprising Ce/H_2O_2, the alloys when immersed in the ~2.9 pH solution, accompanying the dissolution, there also occurs reduction of protons in the acidic solution. Once the interfacial pH is high enough, the $2Ce(OH)_2^{2+}$ species precipitates as CeO_2 as given in the following reaction

$2Ce(OH)_2^{2+} = CeO_2 + 2H^+$ ……..(4)

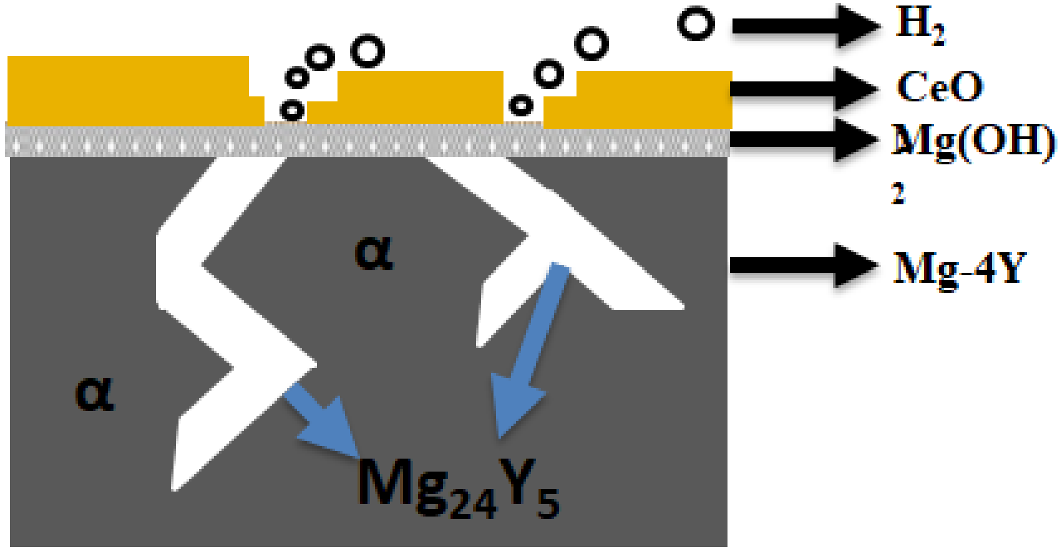

Y.L. Lee et al., "*Applied Surface Science*", 2013, 276: p. 578– 585

Conclusions

Mg-4 wt.% Y alloy was developed y using the bottom pouring squeeze casting set-up.

XRD pattern and EDX confirmed the presence of α-Mg and $Mg_{24}Y_5$ phases in the casted alloy.

The samples of the ingots were coated using the CeCC for different time periods of 30s, 60s, 120s and 1800s.

FESEM-EDX revealed that the Cerium concentration increased with the coating duration and also the coating had been locally damaged with several dry-mud like crisscrossed cracks.

CeCC for 30s demonstrated improved corrosion resistance than the bare and other CeCC coated samples for longer duration during immersion and electrochemical corrosion test.

Reference

1. M. Esmaily et al., "Fundamentals and advances in magnesium alloy corrosion", Progress in Materials Science, 2017, 89: p. 92–193
2. Rong-Gang Hu et al., "Recent progress in corrosion protection of magnesium alloys by organic coatings", Progress in Organic Coatings, 2012, 73: p. 129– 141
3. Carlos E. Castano et al., "Cerium-based oxide coatings", Current Opinion in Solid State and Materials Science, 2015, 19: p. 69–76
4. C. S. Lin and S. K. Fang, "Formation of Cerium Conversion Coatings on AZ31 Magnesium Alloys", Journal of The Electrochemical Society, 2005, 152 (2): p. B54-59
5. F.H. Scholes et al., "The role of hydrogen peroxide in the deposition of cerium-based conversion coatings", Applied Surface Science, 2006, 253: p. 1770–1780
6. W. H. Weber et al., "Raman study of CeO_2. Second-order scattering, lattice dynamics, and particle-size effects", Physical Review B, 1993, 1(48): p. 178-185
7. O. Portillo Moreno et al., "CeO_2 nanoparticles growth by chemical bath and its thermal annealing treatment in air atmosphere", Optik, 2017, 148: p. 142–150
8. Si-Chung Chang, M. Anne Leugers, "Surface Chemistry of Magnesium Oxide-Supported Molybdenum Oxide: An In Situ Raman Spectroscopic Study", J. Phys. Chem. 1992, 96: p. 10358-65
9. Thomas S. Duffy et al., "High-pressure phase transition in brucite, $Mg(OH)_2$", American Mineralogist, 1995, 80: p. 222-230

Thank you